

Supplementary Information for

Spatiotemporal Regulation of Clonogenicity in Colorectal Cancer Xenografts

Authors and affiliations

Maartje van der Heijden¹, Daniël M. Miedema¹, Bartłomiej Waclaw, Veronique L. Veenstra, Maria C. Lecca, Lisanne E. Nijman, Erik van Dijk, Sanne M. van Neerven, Sophie C. Lodestijn, Kristiaan J. Lenos, Nina E. de Groot, Pramudita R. Prasetyanti, Andrea Arricibita Varea, Douglas J. Winton, Jan Paul Medema, Edward Morrissey, Bauke Ylstra, Martin A. Nowak, Maarten F. Bijlsma & Louis Vermeulen*

¹ These authors contributed equally to this work.

*Corresponding author: l.vermeulen@amc.uva.nl

This PDF file includes:

Figs. S1 to S6
Captions for Movies S1 to S3
Caption for Dataset S1
Supplementary methods for Computer models
SI references

Other supplementary materials for this manuscript include the following:

Movies S1 to S3
Dataset S1

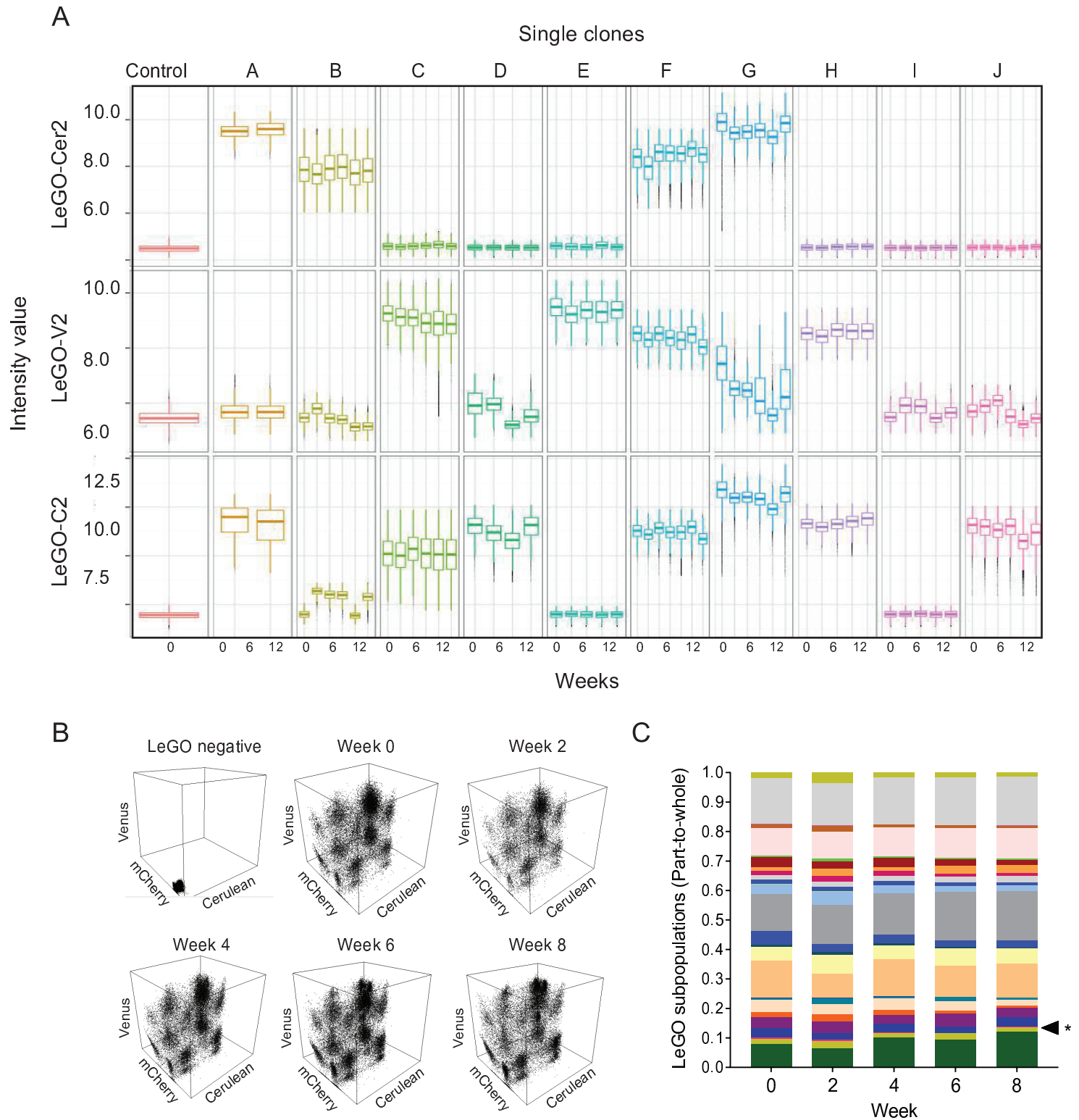


Fig S1 | LeGO vector insertion is stable and overall neutrality is detected in LeGO labeled populations in vitro

(A) Boxplots showing stable fluorescent expression per LeGO vector (vertical axis) for a negative control and 10 single-cloned cell lines (A-J, horizontal axis) derived from LeGO-transduced DLD1 cells. Each boxplot shows a different time point after start of the experiment. LeGO expression for each clone was analyzed by flow cytometry for multiple times within a time range of 12 weeks.

(B) FACs plots are depicting on each axis in 3D the intensity of individual LeGO-transduced DLD1 cells for three vectors: Venus, mCherry and Cerulean. The cell line was analyzed each passage by flow cytometry five times in a ten-week period.

(C) Separate LeGO labelled populations ($n=27$) were analyzed and the graph depicts for each passage the relative contribution of each population. All but one population remained in culture at a stable fraction over the course of this experiment suggesting *grosso modo* neutrality of the LeGO labelled clones. Chi-Square test with Bonferroni correction (* $P < 0.05$).

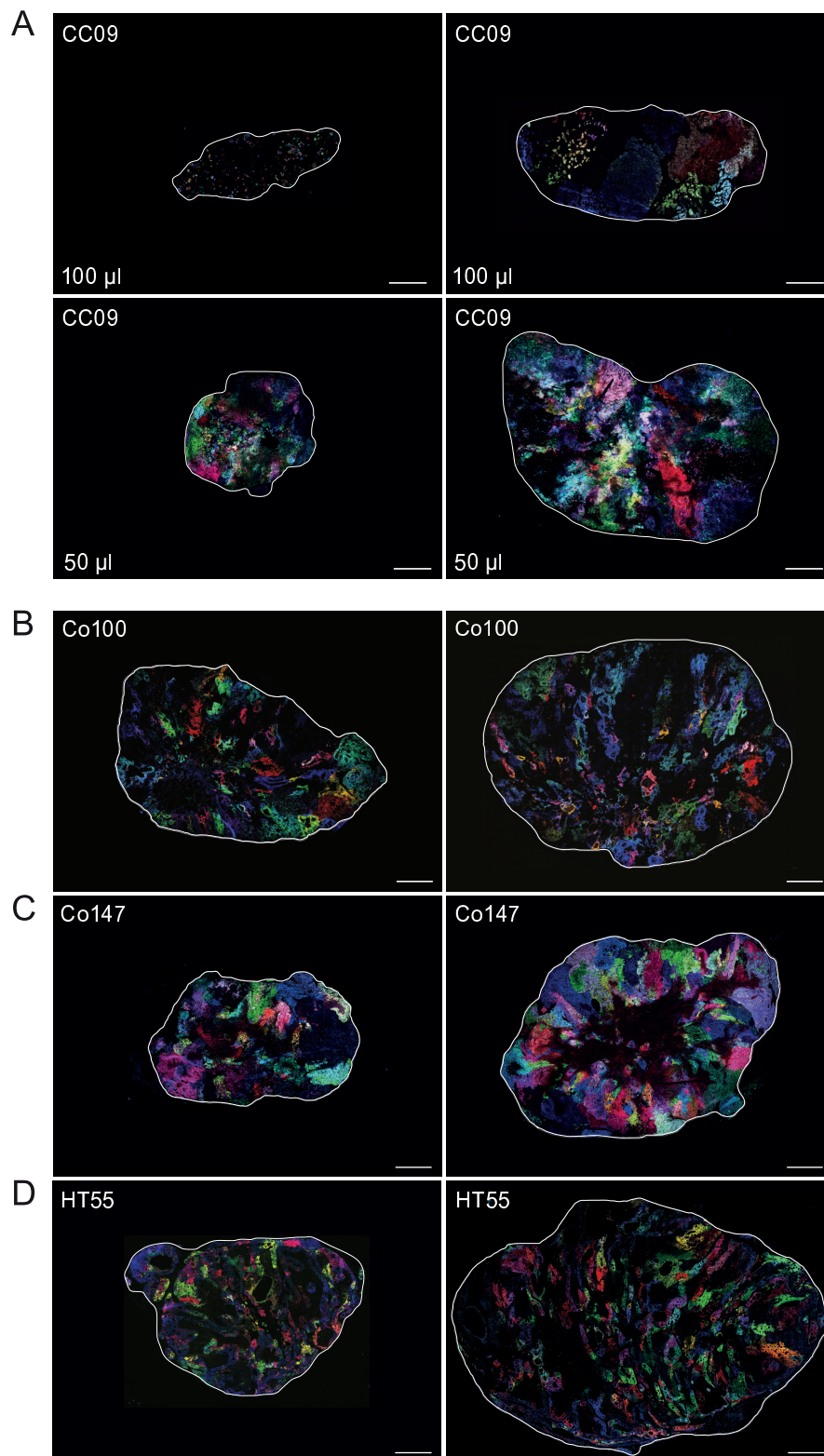


Fig. S2 | Clonal dynamics of LeGO-transduced CRC cells

(A) CC09 tumor isolated at a tumor volume of $\sim 20 \text{ mm}^3$ (upper left panel) and $\sim 70 \text{ mm}^3$ (upper right panel). Tumor cells of the upper panel were injected in a starting volume of 100 mm^3 . CC09 tumor isolated at a tumor volume of $\sim 80 \text{ mm}^3$ (lower left panel) and 360 mm^3 (lower right panel). Tumor cells of the lower panel were injected in a starting volume of 50 mm^3 . Scale bars, 1 mm.

(B) Co100 tumor isolated at a tumor volume of 192 mm^3 (left panel) and Co100 tumor isolated at a tumor volume of 348 mm^3 (right panel). Tumor cells were injected in a starting volume of 50 mm^3 . Scale bars, 1 mm.

(C) Co147 tumor isolated at a tumor volume of 184 mm^3 (left panel) and Co147 tumor isolated at a tumor volume of 231 mm^3 (right panel). Tumor cells were injected in a starting volume of 50 mm^3 . Scale bars, 1 mm.

(D) HT55 tumor isolated at a tumor volume of 173 mm^3 (left panel) and HT55 tumor isolated at a tumor volume of 843 mm^3 (right panel). Tumor cells were injected in a starting volume of 50 mm^3 . Scale bars, 1 mm.

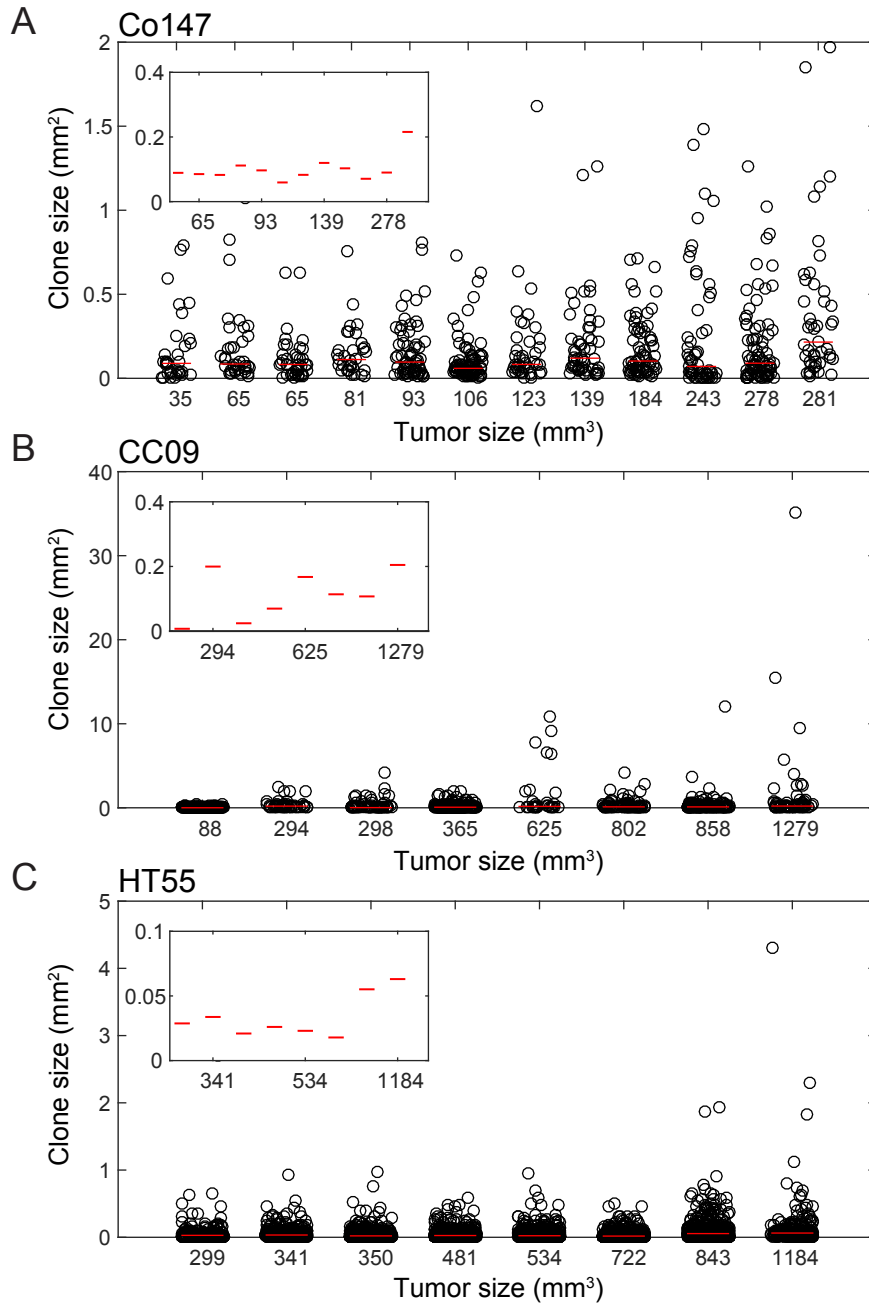


Fig. S3 | Validation of an increased clone size heterogeneity upon tumor growth in multiple colon cancer cell lines

(A-C) Clone sizes per tumor ordered by tumor size for Co147 (upper panel), CC09 (middle panel) and HT55 (lower panel) xenografts. Individual clones (dots) and median clone size per tumor (line). Inset: magnification of median clone sizes.

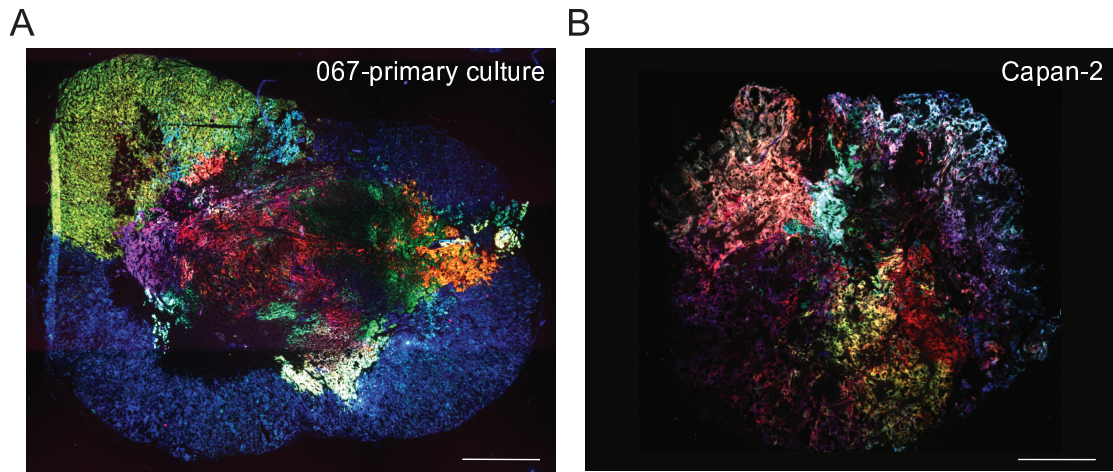


Fig. S4 | Pancreatic ductal adenocarcinoma xenografts display similar growth patterns as CRC
(A) Representative image of a LeGO-transduced primary patient derived pancreatic ductal adenocarcinoma (PDAC) xenograft (067-primary culture). Scale bar, 1 mm.
(B) Representative image of a LeGO-transduced established PDAC culture (Capan-2). Scale bar, 1 mm.

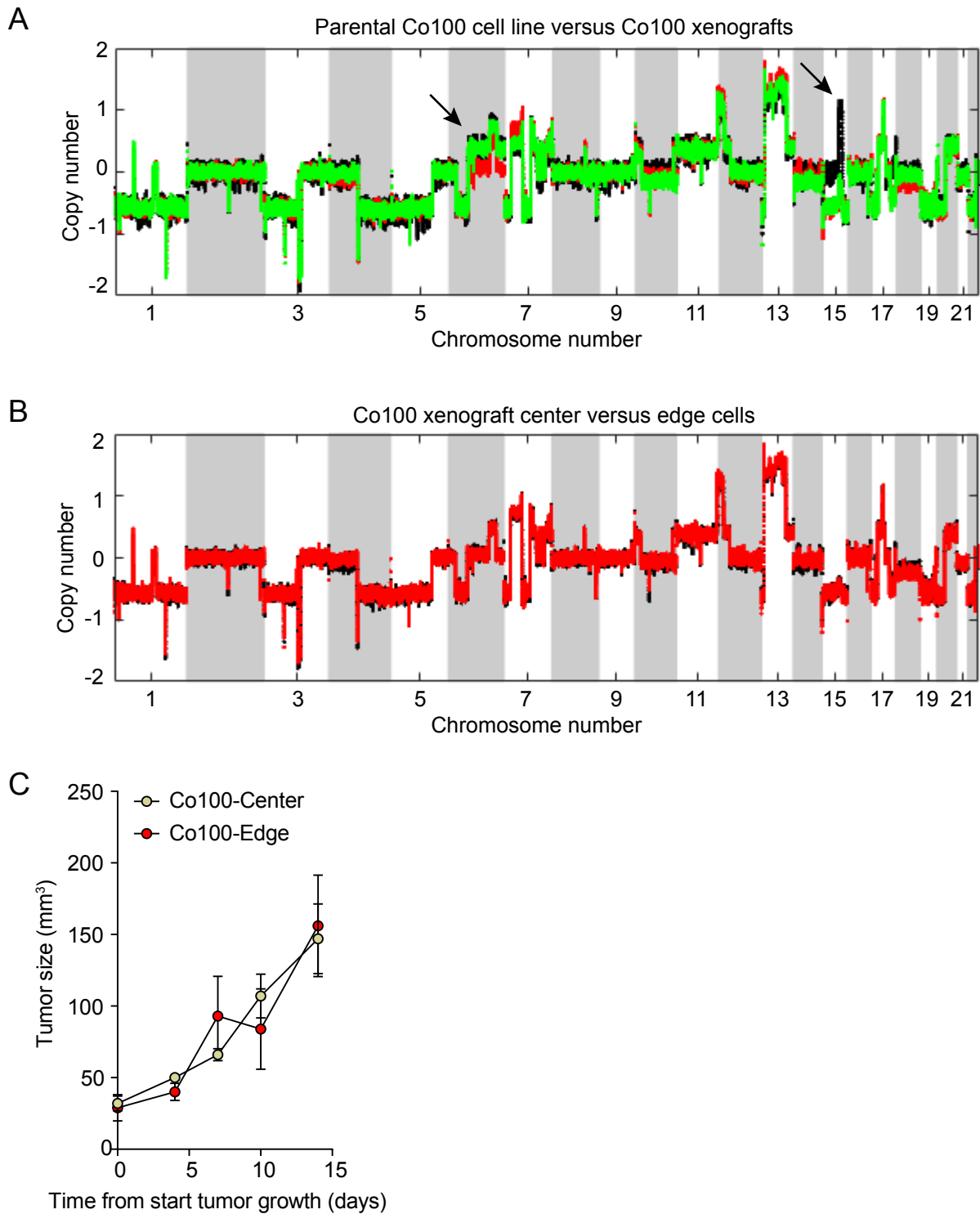


Fig. S5 | Genomic heterogeneity is not underlying the surface growth dynamics of CRC xenografts

(A) Copy number quantification by shallow sequencing is shown for 3 samples of the Co100 line (parental culture in black, and 2 tumors xenografted in the same mouse in red and green). The arrows indicate positions with copy number differences between the samples.

(B) Copy number quantification by shallow sequencing of tumor cells obtained from the center (black) and edge (red) region of a Co100 tumor. No significant copy number differences are observed.

(C) Graph showing the growth curves of tumors derived from Co100 xenografts, either from cells that were previously located in the tumor center (Co100-Center) or on the tumor edge (Co100-Edge), $n=3$ tumors for each group, error bars indicate s.e.m.. Xenografts derived from spatially distinct cell populations display similar growth rates.

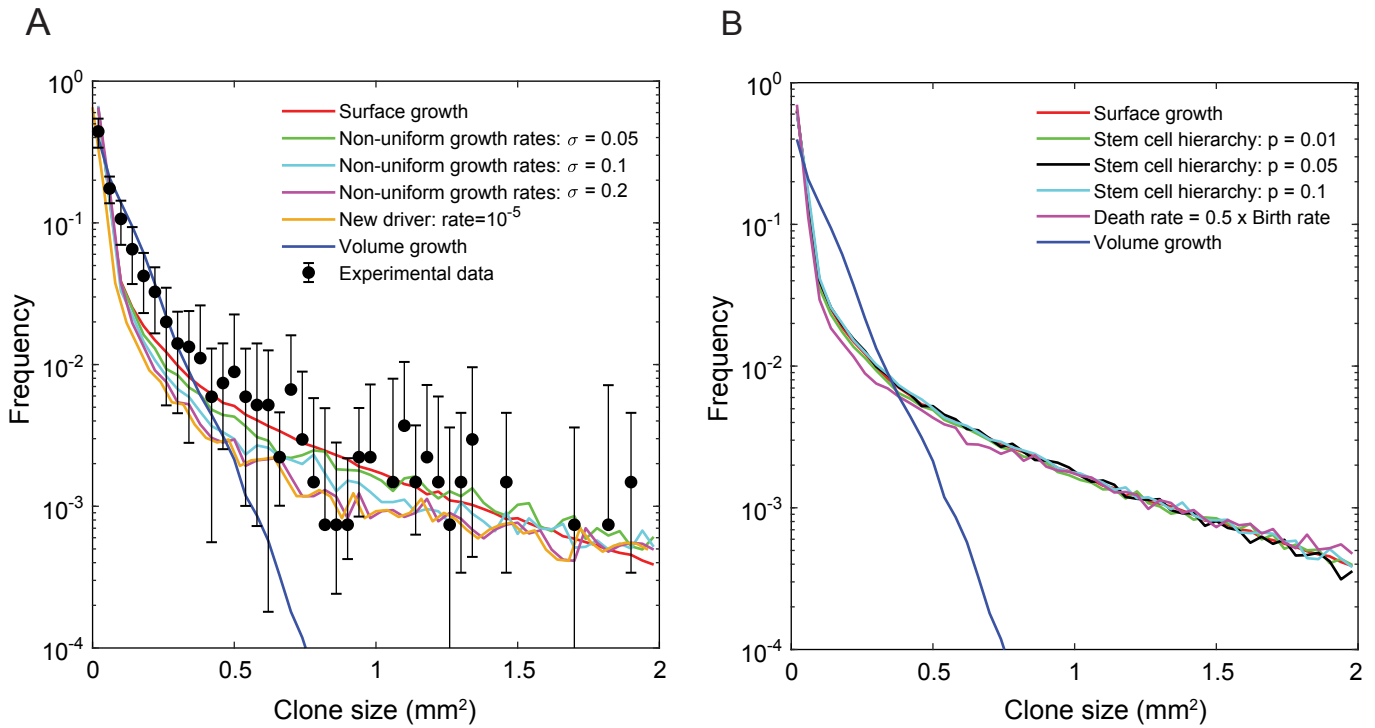


Fig. S6 | Selection or cell hierarchy does not alter the clone size distribution

(A) Distribution of clone sizes from 2D sections of simulated (lines) and experimental tumors (black dots). Simulations are performed with simple surface (red line) or volume growth (blue line) in which all clones have equal growth rates, and with surface growth with non-uniform growth rates. We consider non-uniform growth rates installed at the start of the simulation, with normal distribution of growth rates with standard deviations of $\sigma=0.05$ (green line), 0.1 (cyan line) and 0.2 (magenta line). Mean=1 in all simulations, 6 replicates for each σ . Further, we consider the case where all clones start with equal growth rates, but can acquire a relative increase in growth rate of 10% at each cell division with probability 10^{-5} (orange line).

(B) Graph showing clone size distributions from tumors simulated with simple surface growth (red line), simple volume growth (blue line), surface growth with a stem cell hierarchy (green, black and cyan lines), and surface growth with cell death (magenta line). All clone size distributions from simulations with surface growth are similar, in particular when compared to volume growth.

Movie S1 | Simulation of tumor growth

Sequence of cross-sectional images through the center of a growing tumor simulated with the surface growth model.

Movie S2 | Simulation of growing tumor at various sizes with surface growth model

Animation of a growing tumor with surface growth. The simulation is initiated with 3200 cells distributed randomly in a sphere of volume 3 μl . The final size is 10^8 cells. To better show the dynamics of individual clones, the initial and final size are smaller than in the simulations presented in the main text.

Movie S3 | Simulation of growing tumor at various sizes with volume growth model

Animation of a growing tumor with volume (exponential) growth. The simulation is initiated with 3200 cells distributed randomly in a sphere of volume 3 μl . The final size is 10^8 cells. To better show the dynamics of individual clones, the initial and final size are smaller than in the simulations presented in the main text.

Supplemental Dataset 1 | Clone source data

Table contains all clone sizes (in mm^2) and distance-to-edge per clone (in mm) for all Co100, Co147, CC09 and HT55 xenografts. Data is used for Figure 4 and 5 and Supplemental Figure 4.

Supplementary methods – Computer models

Comparison between experimental and simulated clone size distributions

Definition of the clone size distribution.

Throughout our work, the distribution of clone sizes is measured from the areas of 2D sections of clonal sectors. We note that clones extend in 3D, and therefore the 3D might differ from the 2D distribution. We employed the 2D distribution in our simulations for direct comparison with the experimental data.

Spatial model for tumor growth.

We adapted the spatial model we recently introduced for tumor evolution, for direct comparison with the xenograft data(1). In this model tumor cells occupy sites of a regular 3D lattice. To simulate growth, iteratively a random cell which has at least one of the neighboring sites (Von Neumann neighborhood) vacant, replicates to a randomly chosen vacant neighbor site. This results in growth at the surface (surface growth model). To obtain the volume growth model, in addition to the dynamics described above, cells were moved outwards in the radial direction (\vec{r} to $1.5\vec{r}$, where \vec{r} denotes the position of a cell in 3D space) each time the fraction of cells without free neighboring sites increased above 90%. Technically, this is implemented by counting successful replication attempts for 100 attempted divisions and triggering expansion when the success rate drops below 10%. In both versions of the model, clone identity is installed at the start of a simulation and transferred to all offspring, to mimic the clonal outgrowth of the LeGO marked cells in the xenograft experiments. Tumors are simulated to a maximum size of 1.3 cm^3 (the maximum tumor volume in the experiments), which corresponds to 1.3 billion cells (a cell occupies $1000 \text{ }\mu\text{m}^3$).

Non-neutral model.

We investigated how sensitive the observed clone size distribution is to selective differences between clones. We repeated our simulations with each of the 10000 initial cells having a unique growth rate drawn from a normal distribution with mean =1 and three different standard deviations ($\sigma = 0.05, 0.1, 0.2$). The ratio of the growth rates of the fittest to the least fit clone could be as large as 6 for $\sigma = 0.2$, and 2.2 for $\sigma = 0.1$. We note that since we always compare tumors of the same size rather than growth time, only relative differences in the growth rate matter and hence we are permitted to choose the mean growth rate to be one for convenience.

We found that the clone size distribution for all σ 's was heavy-tailed and very similar to the neutral case in which all clones have equal growth rate (**Fig. S7A**). Even in the case of $\sigma = 0.2$, which corresponds to unrealistically large fitness differences, the clone size distribution deviates very little from surface growth with uniform growth rates, and is significantly different from the narrow distribution obtained in the volume growth model.

We also investigated a surface growth model in which all clones have initially the same fitness, but they can acquire new drivers (modelled as a 10% increase in growth rate) with probability 10^{-5} per cell division. Again, we observed no significant deviation from the neutral case (**Fig. S7A**).

Model with cell death.

To test if cell death has an impact on the distribution of clone sizes, we extended our surface growth model to include random death of any cell. Cells die and are removed with rate $d = 0.5b$, where $b = 1$ is replication rate. Death creates space for adjacent cells to divide, also in the bulk of the tumor. **Fig. S7B** shows that the clone size distribution is altered only very slightly compared to simulations without cell death.

Model with cell hierarchy.

We also extended the surface growth model to include loss of clonogenicity resulting from intrinsic (stem cell differentiation) processes. In this hierarchical version of the model, adopted from Poleszczuk et al., cells stop growing if there is no more free space in the immediate surrounding or if a cell division resulted in two non-clonogenic (with probability p) cells instead of two clonogenic cells (probability $1-p$)(2). Similar to cell death, also a stem cell hierarchy has minimal impact on the distribution of clone sizes for surface growth (**Fig. S7B**).

Calculation of the simulated clone size distribution.

For each tumor simulated in 3D, five 2D cross sections are taken at positions $z = 0, \pm r/3, \pm 2r/3$ (where r is tumor radius) and we determined the positions and sizes of all clones. We rejected clones smaller than 50 cells as this is the minimum size we can detect experimentally. We repeated the above procedure for all simulated sizes $10^8, 2 \times 10^8, \dots, 13 \times 10^8$, and pooled the data. We then calculated the size of each clone in mm^2 by multiplying the number of cells by 10^{-4}mm^2 (average area of a single cell). We binned the data according to clone area (bin width = 0.04mm^2) and calculated the number of events in each bin. We normalized the obtained histogram (clone size distribution) by dividing the number of events in each bin by the total number of observed clones with a size larger than 50 cells, so that the numbers on the vertical axis of e.g. **Fig. 5C** represent probabilities of finding a clone whose size falls into a particular bin.

We note that pooling the data corresponding to a linear range of tumor sizes assumes that tumor sizes are uniformly distributed between 100, 200...1300 mm^3 . The experimental tumor volumes are not entirely uniformly distributed over this range. However, we checked that using the experimental distribution of tumor sizes does not significantly affect the obtained clone size distribution.

References

1. B. Waclaw *et al.*, A spatial model predicts that dispersal and cell turnover limit intratumour heterogeneity. *Nature* **525**, 261-264 (2015).
2. J. Poleszczuk, P. Hahnfeldt, H. Enderling, Evolution and phenotypic selection of cancer stem cells. *PLoS Comput Biol* **11**, e1004025 (2015).